

Research paper

## Functional connectivity analysis of the depression connectome provides potential markers and targets for transcranial magnetic stimulation

Hugh Taylor<sup>a</sup>, Peter Nicholas<sup>a</sup>, Kate Hoy<sup>b,c</sup>, Neil Bailey<sup>b,d,e</sup>, Onur Tanglay<sup>a</sup>,  
Isabella M. Young<sup>a</sup>, Lewis Dobbin<sup>a</sup>, Stephane Doyen<sup>a</sup>, Michael E. Sughrue<sup>a,\*</sup>,  
Paul B. Fitzgerald<sup>e</sup>

<sup>a</sup> Omniscient Neurotechnology, Sydney, Australia

<sup>b</sup> Central Clinical School Department of Psychiatry, Monash University, Camberwell, Victoria, Australia

<sup>c</sup> Bionics Institute, 384-388 Albert St, East Melbourne, Vic 3002, Australia

<sup>d</sup> Monarch Research Institute Monarch Mental Health Group, Sydney, New South Wales, Australia

<sup>e</sup> School of Medicine and Psychology, The Australian National University, Canberra, ACT, Australia



### ARTICLE INFO

#### Keywords:

Connectivity  
Machine learning  
Depression  
Treatment response

### ABSTRACT

**Background:** Despite efforts to improve targeting accuracy of the dorsolateral prefrontal cortex (DLPFC) as a repetitive transcranial magnetic stimulation (rTMS) target for Major Depressive Disorder (MDD), the heterogeneity in clinical response remains unexplained.

**Objective:** We sought to compare the patterns of functional connectivity from the DLPFC treatment site in patients with MDD who were TMS responders to those who were TMS non-responders.

**Methods:** Baseline anatomical T1 magnetic resonance imaging (MRI), resting-state functional MRI, and diffusion weighted imaging scans were obtained from 37 participants before they underwent a course of rTMS to left Brodmann area 46. A novel machine learning method was utilized to identify brain regions associated with each item of the Beck's Depression Inventory II (BDI-II), and for 26 participants who underwent rTMS treatment over the left Brodmann area 46, identify regions differentiating rTMS responders and non-responders.

**Results:** Nine parcels of the Human Connectome Project Multimodal Parcellation Atlas matched to at least three items of the Beck's Depression Inventory II (BDI-II) as predictors of response to rTMS, with many in the temporal, parietal and cingulate cortices. Additionally, pre-treatment mapping for 17 items of the BDI-II demonstrated significant variability in symptom to parcel mapping. When parcels associated with symptom presence and symptom resolution were compared, 15 parcels were uniquely associated with resolution (potential targets), and 12 parcels were associated with both symptom presence and resolution (blockers or biomarkers).

**Conclusions:** Machine learning approaches show promise for the development of pathoanatomical diagnosis and treatment algorithms for MDD. Prospective studies are required to facilitate clinical translation.

### 1. Introduction

Repetitive transcranial magnetic stimulation (rTMS) is recognized as an effective intervention for patients with major depressive disorder (MDD), particularly for patients resistant to first-line treatments (Amad and Fovet, 2022). While a substantial body of evidence supports the superiority of rTMS treatment applied to the left dorsolateral prefrontal cortex (DLPFC) compared to sham treatment, only 30–60 % of patients with treatment resistant MDD show a clinically meaningful response, with an estimated 10–60 % reduction in overall symptom burden (Ma

et al., 2010). Currently, it remains unclear which individual factors contribute to the heterogeneity in clinical response (Beuzon et al., 2017; Hasanzadeh et al., 2019; Kaster et al., 2019), making it difficult to predict clinical outcomes and identify potential candidates.

While rTMS is a useful tool for difficult patient populations, several interconnected ideas about how to improve the success rate have been proposed. In addition to improving the selection of stimulation parameters (Gellersen and Kedzior, 2019; Risio et al., 2020), improving the targeting accuracy of the stimulation (e.g., more accurately targeting the DLPFC) appears to be a highly promising approach (Cash et al., 2021;

\* Corresponding author at: Omniscient Neurotechnology, Level 10, 580 George St, Sydney, NSW, Australia.

E-mail address: [sughruevs@gmail.com](mailto:sughruevs@gmail.com) (M.E. Sughrue).

<https://doi.org/10.1016/j.jad.2023.02.082>

Received 19 July 2022; Received in revised form 2 February 2023; Accepted 19 February 2023

Available online 24 February 2023

0165-0327/© 2023 Elsevier B.V. All rights reserved.

Fitzgerald, 2021). Several studies have demonstrated that the use of image-based guidance to improve accuracy does have the potential to provide beneficial clinical outcomes when compared to guidance based on craniometric measurements (i.e. the “5-cm rule”) (Cash et al., 2021; Fitzgerald et al., 2009). Furthermore, even when using image-based guidance to visually ensure the stimulation target is located within the DLPFC, a more granular approach to targeting the correct portion of the DLPFC might be necessary. Previous studies have demonstrated that rTMS induces changes in functional connectivity (Corlier et al., 2019), and functional connectivity may be used to predict rTMS outcome. The Human Connectome project (Glasser et al., 2016), and others (Cieslik et al., 2013; Muhle-Karbe et al., 2016), have noted that the DLPFC is made up of dozens of unique subregions, or parcels, each of which are components of different large scale brain networks, wherein their connectome classification may differ from their immediate neighboring subregion within the DLPFC (Yeo et al., 2011). An increased degree of granularity in targeting may also be necessary for optimal clinical results, as targeting a portion of the DLPFC outside of Brodmann's area 46 seems to lessen efficacy as a depression treatment (Rosen et al., 2021).

Accurate target selection may also require a personalized approach based on both symptomatology and functional connectivity. If this is the case, it may underlie the observed heterogeneity in clinical outcomes (Siddiqi et al., 2019). This study used a novel machine learning method, the Hollow-tree Super (HoTS) method, to address two hypotheses. Following the identification of the exact location of the stimulation on the parcellated brain, we first expected that patients with MDD who were TMS responders would show distinct patterns of functional connectivity compared to TMS non-responders. Second, we mapped the different symptom profiles within all patients (responders and non-responders to rTMS) to different patterns of pretreatment functional connectivity. This approach aimed to determine which regions outside the left DLPFC might explain the symptom heterogeneity seen in these patients, and their responses to the intervention (Blom et al., 2014; Dalglish et al., 2020; Drysdale et al., 2017), which might present novel targets for stimulation. Together, we believe these data will provide insight into the role of functional connectivity-based analysis in improved response prediction, novel target selection, and possibly direct symptom specific target selection.

## 2. Methods and materials

### 2.1. Patient cohort

37 participants with a diagnosis of MDD underwent T1 and T2 magnetic resonance imaging (MRI), resting-state functional MRI (rsfMRI), and diffusion weighted imaging (DWI) (Table 1). These participants were part of a larger clinical study (Australian and New Zealand Clinical Trials Registry: Investigating Predictors of Response to Transcranial Magnetic Stimulation for the Treatment of Depression; ACTRN12610001071011; <https://www.anzctr.org.au/Trial/Registration/TrialReview.aspx?id=336262>). Although the original dataset had 39 participants who underwent rTMS, tractography could not be reconstructed in two participants. Depression symptom severity was assessed using the Hamilton Depression Rating Scale (HAM-D), the Montgomery-Asberg Depression Rating Scale (MADRS), and Beck's Depression Inventory (BDI-II).

### 2.2. rTMS protocol

After depression severity assessment, individuals initially completed 3 weeks of rTMS to the left DLPFC (10 Hz, daily Monday through Friday) (Bailey et al., 2018), targeted using the F3 Beam approach (Beam et al., 2009). If they do not respond within 3-weeks, they were randomized to either continue the same treatment, crossover to 10 Hz rTMS to the right DLPFC or sequential bilateral rTMS. Due to the inclusion of the crossover condition, our results should be viewed as a test of the association

**Table 1**  
Subject demographics.

N	37
Age (mean ± SD)	42.9 ± 12.8
Sex (M/F)	21/16
Age of onset (mean ± SD)	25.7 ± 11.0
Length of illness (mean ± SD)	19.4 ± 11.6
MADRS <sup>a</sup> (mean ± SD)	
Baseline	33.2 ± 6.7
Week 3	29.0 ± 8.9
Week 6	25.2 ± 10.8
rTMS responders <sup>b</sup> (%)	27.0
BDI <sup>c</sup> (mean ± SD)	
Baseline	34.0 ± 9.2
Week 3	28.0 ± 11.1
Week 6	23.8 ± 12.8
Medications <sup>d</sup>	
Antidepressants, n	
SSRI	8
SNRI	5
Other	13
Benzodiazepines, n	14
Antipsychotics, n	14
Mood stabilizers, n	4

<sup>a</sup> Montgomery-Asberg Depression Rating Scale, range of possible scores 0 to 60.

<sup>b</sup> Clinical response defined as 50 % reduction in total MADRS score. This was not the criterion used for analysis.

<sup>c</sup> Beck's Depression Inventory, range of possible scores 0 to 63.

<sup>d</sup> 12 patients were taking >1 medication from a single class. 15 patients were taking a combination of treatments (i.e. one or more medications from at least two of the antidepressant, benzodiazepine, antipsychotic, or mood stabilizer categories).

between brain regions associated with specific BDI items during rTMS in general, rather than a specific rTMS treatment location, as both 1 Hz rTMS to the right DLPFC and sequential bilateral rTMS have demonstrated efficacy (Cao et al., 2018; Fitzgerald et al., 2006). Response criteria followed through from a previous study (Australian and New Zealand Clinical Trials Registry: Investigating Predictors of Response to Transcranial Magnetic Stimulation for the Treatment of Depression; ACTRN12610001071011; <https://www.anzctr.org.au/Trial/Registration/TrialReview.aspx?id=336262>), where response was defined as a 50 % reduction on the Hamilton Depression Rating Scale (HAM-D). However, in the present study, for the purpose of integrating the data into our ML method, response to treatment was defined by creating a reliable change index (RCI) per subject to categorize into responders vs. non-responders based on their scores on the BDI-II. Simulation coordinates were reconstructed using combined T1 and T2 scans and converted from native to standard space using.

FSL Version 5.0.10 software (Jenkinson et al., 2012) and customized MATLAB R2017a scripts (The Math-Works, Inc., Natick, MA). As per the methodology of our previous rTMS-specific study, assessment with the BDI-II, MADRS and HAM-D was repeated following treatment at 3 weeks from baseline, and then at 6 weeks from baseline. However, for the purpose of our present study, analysis was only done with the BDI-II items, to allow for mapping of symptomatology to brain regions. Furthermore, as mentioned previously, a RCI was used to categorize participants into responders vs non-responders. While analysis on baseline BDI-II items was performed on the entire dataset of 37 participants, analysis on brain regions associated with symptom resolution following rTMS was only carried out on participants if their target site was validated to be left BA46, as defined by the Human Connectome Project Multimodal Parcellation (HCP-MMP1) atlas (Glasser et al., 2016). This manifested in a subgroup of 26 participants.

### 2.3. Imaging protocol

All patients underwent diffusion tractography images with the

following parameters: Siemens Magnetom Trio 3 T MRI scanner, with 10 b = 0 baseline image and a b = 1000 shell with 60 direction acquisition and 2 mm isotropic voxels.

We also acquired a resting-state fMRI with the following parameters:  $3.5 \times 3.5 \times 3.3$  mm voxels, TR = 2000 ms, TE = 25 ms, 200 volumes/run.

#### 2.4. Diffusion tractography preprocessing steps

The diffusion weighted imaging (DWI) was processed using the Omniscient software, which employs standard processing steps in the Python language. The processing pipeline includes the following steps: 1) the diffusion image is resliced to ensure isotropic voxels, 2) motion correction is performed using a rigid body registration algorithm to a baseline scan, 2) slices with excess movement (defined as DVARS > 2 sigma from the mean slice) are eliminated, 3) the T1 image is skull stripped using the HD-BET software (25), which is inverted and aligned to the DT image using a rigid alignment, and this aligned T1 image is then used as a mask to skull strip the aligned DT image, 4) gradient distortion correction is performed by applying a diffeomorphic warping registration method between the DT and T1 images, 5) The fiber response function is estimated and the diffusion tensors are calculated using constrained spherical deconvolution, 7) deterministic tractography is performed with uniform random seeding, 4 seeds per voxel, usually creating about 300,000 streamlines per brain.

#### 2.5. Creation of a personalized brain atlas using machine learning based parcellation

In order to minimize the effects of gyral variation, a machine learning based, subject specific version of the HCP-MM1 atlas was generated using each subject's structural connectivity by warping the HCP atlas onto each individual's brain based on structural connectivity, based on the methodology recently described by our group (Doyen et al., 2022). This method created a version of the HCP-MMP1 atlas with 181 cortical parcels along with 8 subcortical structures per hemisphere, along with the brainstem as one parcel.

#### 2.6. rsfMRI preprocessing steps

The rsfMRI images were processed using standard processing steps. 1) motion correction on the T1 and BOLD images was performed using a rigid body alignment; 2) slices with excess movement (defined as DVARS > 2 sigma from the mean slice) were eliminated; 3) skull stripping was performed on the T1 image using a convolutional neural net (CNN), which was inverted and aligned to the resting state bold image using a rigid alignment, and used as a mask to skull strip the rsfMRI image; 4) slice timing was corrected; 5) Global intensity normalization was performed; 6) gradient distortion was corrected using a diffeomorphic warping method to register the rsfMRI and T1 images; 7) High variance confounds were calculated using the CompCor method (Behzadi et al., 2007). These confounds as well as motion confounds were regressed out of the rsfMRI image, and the linear and quadratic signals were detrended. Note, this method does not perform global signal regression; 8) spatial smoothing was performed using a 4 mm FWHM Gaussian kernel. The personalized atlas created in previous steps was registered to the T1 image, and grey matter atlas regions were aligned with the grey matter regions in each participant's scans. Thus, the personalized atlas was ideally positioned for extracting a BOLD time series, averaged over all voxels within a region, from all 379 regions. The Pearson correlation coefficient was calculated between the BOLD signals of each unique area pair (self to self-inclusive), which yielded 143,641 correlations.

#### 2.7. Mapping of symptoms to brain regions using the Hollow-tree Super (HoTS) method

The black box problem in machine learning encompasses the inability to gain visibility into the processes performed on inputs of a machine learning model to compute the output. This limits the potential for the results of machine learning research to transition into clinical practice, because for results to provide meaningful insights into rTMS targeting in clinical practice there is a need to know which part of the brain is generating a problem, and as such could be targeted for symptom improvement. For this reason, we used a boosted trees approach, called Hollow-tree Super (HoTS) (Doyen et al., 2021) which is a useful computational tool for making inferences on datasets. In this case, we used it specifically to obtain information about which features the model was using for its outputs. These features provided insight into which brain regions showed functional connectivity which was linked to the symptom or its treatment response.

In this study, the HoTS method was used to find the regions with connectivity values that most contributed to exploring: 1) pre-treatment presence or absence of a BDI-II item, with presence defined as a response score equal to or > 2 for each questionnaire item, 2) overall response to rTMS at left area 46, with resolution defined as having the symptom present pre-treatment, and not present post-treatment, at 6 weeks from baseline. Cut-offs for symptom presence and improvement for the machine learning analyses were defined as a 50 % reduction in score on the BDI-II item measure. A score > 2 indicated more severe symptoms and was clearly differentiable from participants for whom the BDI-II item did not apply. Similarly, we opted to use BDI-II scores as the models were able to achieve a relatively high area under the curve (AUC) for the presence and improvement of almost all BDI-II items. Only cases with an AUC above 0.7 were included in the final results. Identified parcels were mapped to known resting-state networks of the Yebo-Buckner atlas (Akiki and Abdallah, 2019; Yebo et al., 2011): the Default Mode Network (DMN), the Central Executive Network (CEN; also referred to as the Frontoparietal Network), the Dorsal Attention Network (DAN), Salience Network (SN), Sensorimotor Network (SMN), Limbic Network (LN), and Visual Network (VN).

#### 2.8. The parcel level consistency of image guided targeting

We performed structural connectivity based atlasing to utilize the diffusion tractography imaging, allowing the adjustment of boundaries of the HCP-MMP1 atlas to fit each patient's structural connectivity. Using the stored coordinates of the treatment site performed for each patient, we then compared the parcel treated and found that left area 46 was the target at the center of the field in 67 % of cases ( $n = 26$ ; Fig. 1). The other stimulation sites were located in neighboring parcels: specifically left a9-46v, left p9-46v, left 9-46d, left 9a, and left 9p. While these are minor differences in spatial location, these differences mean that in two cases, the therapy was centered over a different large scale brain network, as left a9-46v and left p9-46v are typically found to be functionally part of the central executive network (16, 32). As such, subsequent analysis on predictors of response to rTMS was performed on the cohort of patients who received rTMS to area left 46 ( $n = 26$ ). Despite the small sample size, we were able to produce a model for most items of the BDI-II with a high AUC. Furthermore, this small sample was permissible in the context of creating a model as it was focused only on the sample of 26, rather than creating an extrapolation tool for predicting population responses to TMS treatment. To prevent over-fitting, a common by-product of training a model on a small sample size, we used 5-fold cross-validation to reduce the impact of this on its ability to make inferences on the sample it was trained on.

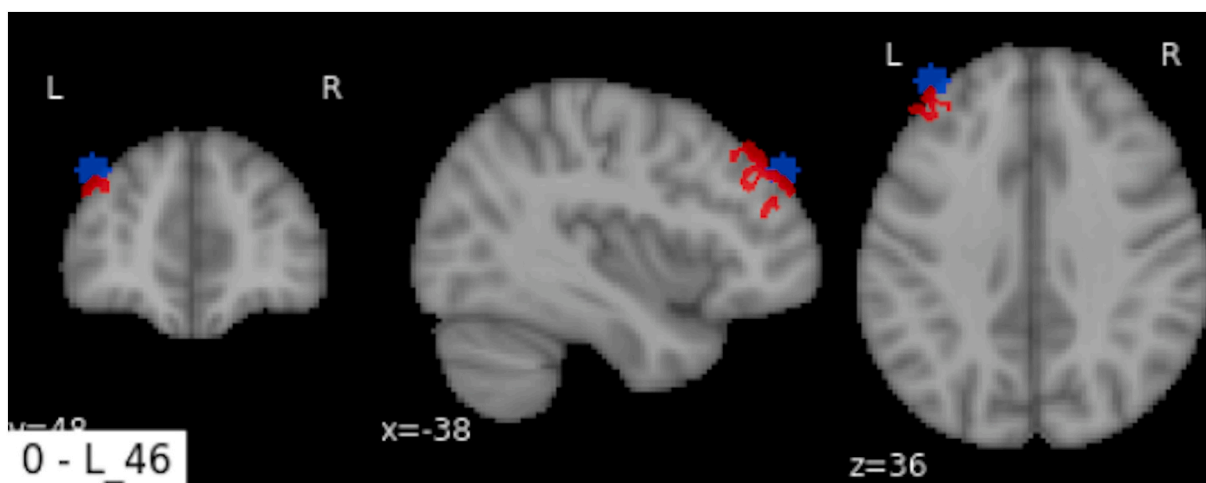


**Fig. 1.** The stored coordinates from Transcranial Magnetic Stimulation treatments of the left dorsolateral prefrontal cortex (average pictured in blue) was compared to left area 46 (red) which was the target at the centre of the field in 67 % of cases. (For interpretation of the references to colour in this figure legend, the reader is referred to the web version of this article.)

### 3. Results

#### 3.1. Predictors of response to left BA46 rTMS

Within the group of patients who received treatment stimulation to left BA46 ( $n = 26$ ), the HoTS method was used to identify baseline functional connectivity features associated with the resolution of symptoms following rTMS, defined as complete absence of symptoms post-treatment (a BDI-II score of 0 for that specific BDI-II item). This included patients who participated in the crossover condition. Models for 19 BDI-II items met the AUC threshold of 0.7 (Fig. 2a). Across the models for each symptom, the method identified 169 parcels that predicted BDI-II item resolution following rTMS. The full list of predictors, along with log odds predicted by the model can be found in Supplementary Table 1 and Supplementary Figs. 1–21.

The functional connectivity features of the 169 parcels were used by the machine learning models to predict resolution of BDI-II items. These represented 127 distinct parcels which were used in at least one model to predict resolution of at least one item of the BDI-II, as 29 parcels were apparent in  $>1$  model. The resolution of a given item could result in the model demonstrating an increased correlation of a specific parcel with other regions, decreased correlation with other regions, or a mixture of both. While connectivity features of 98 parcels were associated with resolution of a single BDI-II item, 29 parcels were associated with resolution of at least two BDI-II items (Fig. 2b). Out of the total 127 parcels associated with BDI-II item resolution, 30 parcels were affiliated to the DMN, 24 to the SMN, 22 to the VN, 17 to the CEN, 11 to the DAN, 11 to the SN, 5 to the LN, and 7 parcels were subcortical structures (Fig. 2c). We next decided to focus only on parcels associated with resolution at least three BDI-II items to increase the sensitivity of the association between symptom resolution and network connectivity. Nine parcels were associated with resolution of three or more items of the Beck's Depression Inventory (Fig. 2d). Out of these nine parcels, four were associated with the DMN (left 31 pv, left STSda, right v23ab, right STGa), two with the SMN (left 1, left 3b), one with the VN (right TPOJ3), one with the DAN (left PFT), and one was a subcortical structure (right Thalamus).

#### 3.2. Symptom to parcel mapping

We next performed HoTS based analysis on rsfMRI acquired prior to treatment against baseline items of the BDI-II to obtain a symptom-based parcel map, where having a symptom was defined as a score equal to or

$>2$  on each item. This was performed on the entire cohort of 37 participants. Models for 16 symptoms met the AUC threshold of 0.7 (Fig. 3a). Similar to the model constructed from the associations between symptom resolution and baseline connectivity, most parcels were matched to a single BDI-II item, and 27 were matched to at least two items (Fig. 3b). There was however significant heterogeneity in network affiliations of parcels associated with each symptom and we were unable to discern clear clusters (Fig. 3c). We then focused on parcels associated with at least two BDI-II items in order to identify key parcels which may provide further targets for rTMS. Of these 27 parcels, 6 were affiliated with the DMN, 6 with the CEN, 4 with the SMN, 3 with the VN, 3 with the DAN, 1 with the SN, and 4 parcels were subcortical structures (Fig. 3d). The full results of the parcel to symptom map, along with log odds predicted by the model can be found in Supplementary Table 2 and Supplementary Figs. 1–21.

#### 3.3. Predictors of both symptom presence and TMS response reveal additional therapeutic markers

Finally, to understand the role of response predictors identified by the machine learning model, we examined the overlaps between predictors of response and predictors of symptom presence (Fig. 4a). In order to identify pertinent patterns, we examined the set of 27 parcels explaining response to two or more BDI-II items. 15 out of 27 parcels were only associated with symptom resolution (Fig. 4b). Among these, six were associated with the DMN (left 47 m, left A5, left 9p, left 31 pv, right STGa, right v23ab), three with the SMN (left 2, left A5, right 24dv), two with the VN (right TPOJ3, left IPO), two with the DAN (right TE2p, left PFT), one with the CEN (left IFSa), one with the SN (left 46) and one was a subcortical structure (right Accumbens). The rest of the 14 parcels were predictors of both symptom resolution and symptom presence at baseline (Fig. 4a). Four of these were affiliated with the DMN (right 47 m, right d23ab, right 8Ad, left STSda), three with SMN (right 6mp, left 3b, left 1), two with VN (right LO2, left FST), two with CEN (left RSC, right 7Pm), two with SN (left FOP1, right PBelt), and one was a subcortical structure (right Thalamus). Next, we further examined parcels that predicted both the presence of a symptom and resolution of the same symptom (Fig. 4c). Six BDI-II items had the same predictor for presence and resolution, mapping to ten parcels (Fig. 4c-d).

### 4. Discussion

Given the 30–60 % response rates to rTMS to the left DLPFC, it is

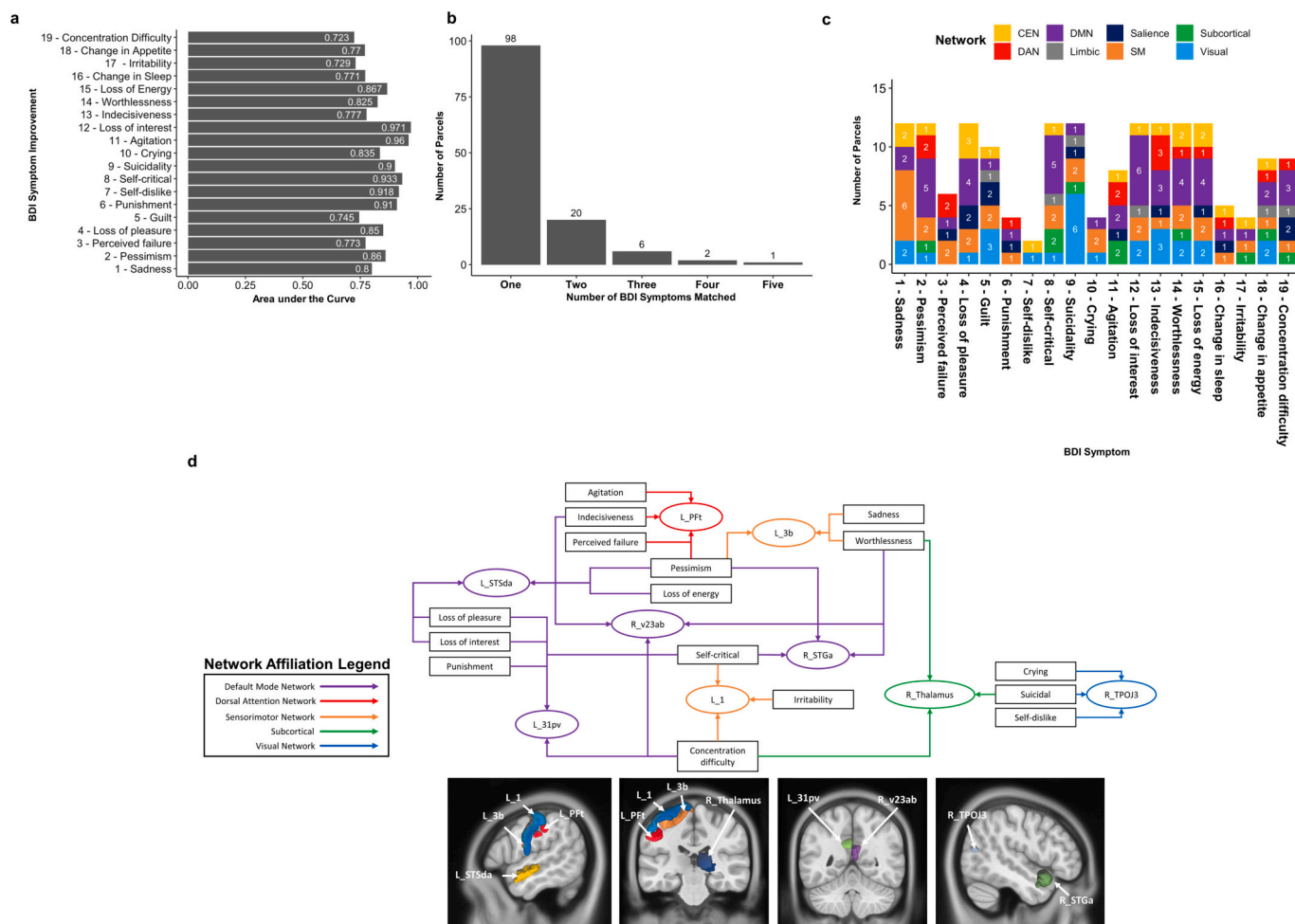


**Fig. 2.** Baseline resting-state fMRI parcels predict response to repetitive Transcranial Magnetic Stimulation treatment. (a) When a complete absence of symptoms post-treatment was defined as response to treatment, 19 items of the Beck's Depression Inventory surpassed the AUC threshold of 0.7. (b) Further analysis demonstrated the number of parcels that were associated to each symptom the Beck's Depression Inventory measured. The graph depicts the number of parcels that are associated with one, two, three or more symptoms. It demonstrates there are 9 parcels that were matched to at least three symptoms, which identifies the parcels with the most pertinent patterns. (c) A graphical representation of the network affiliation of each parcel that is associated with a symptom on the Beck's Depression Inventory. The graph plots 169 parcels, rather than 127, as it includes the duplicates of the 29 parcels which matched to multiple symptoms. Some symptoms had a larger representation of networks compared to others. (d) A symptom to parcel map of the nine parcels associated with resolution of at least three symptoms, along with their anatomical location on T1-weighted magnetic resonance imaging. The colors of the arrows represent their network affiliations. DMN, Default Mode Network; SM, Sensorimotor Network; blue, DAN, Dorsal Attention Network; CEN, Central Executive Network. (For interpretation of the references to colour in this figure legend, the reader is referred to the web version of this article.)

worth addressing the notable possibility that we lack adequate methods for identifying appropriate stimulation target candidates. Data driven approaches to both response prediction for rTMS treatment and treatment parameters could improve identification of patients who should be treated using rTMS and enhance treatment efficacy through optimal rTMS targeting. It is possible that different symptoms in MDD might be associated with different functional connectivity abnormalities in different neural circuits, and thus different rTMS targets might result in improvement in different symptoms, via changes in connectivity of different large-scale networks. We demonstrate the presence of multiple symptom predictors: anatomical regions associated with the presence of multiple symptoms, regions associated with resolution of these symptoms, and in some cases, regions associated with both the symptoms and prediction of resolution of that symptom. We propose that these regions may serve as potential secondary targets for rTMS treatment, or as markers of rTMS response. Ultimately, machine learning approaches show promise for pathoanatomy-based diagnosis and treatment of mental illnesses like MDD.

The optimal target for rTMS treatment of major depression remains

unclear. Studies relying on the 5 cm method have been shown to target inconsistent clusters within the DLPFC (Fitzgerald, 2021; Li et al., 2017). In contrast, a more recent approach relied on functional connectivity to identify the subregion in the DLPFC that is most anti-correlated with the subgenual anterior cingulate cortex (SGC) (Cash et al., 2019; Fox et al., 2012; Weigand et al., 2018). Targeting that is closer to the target recommended by this method is strongly correlated with treatment response, though prospective randomized data is lacking. Nonetheless, the treatment site identified through this method was more anterior and lateral when compared to those identified using the 5 cm method, which may partly explain the improved treatment response from targeting that more closely approximates the site recommended by this method. Alternatively, stimulation at two separate targets within the DLPFC may address two separate clusters of symptoms. Anterolateral stimulation has been shown to be best for dysphoric symptoms, while posteromedial stimulation improved anxiousomatic symptoms (Siddiqi et al., 2019). This separation in the association between treatment site and specific symptom sub-type response is not especially surprising given that the boundaries of large-scale brain networks are often sharp and adjacent



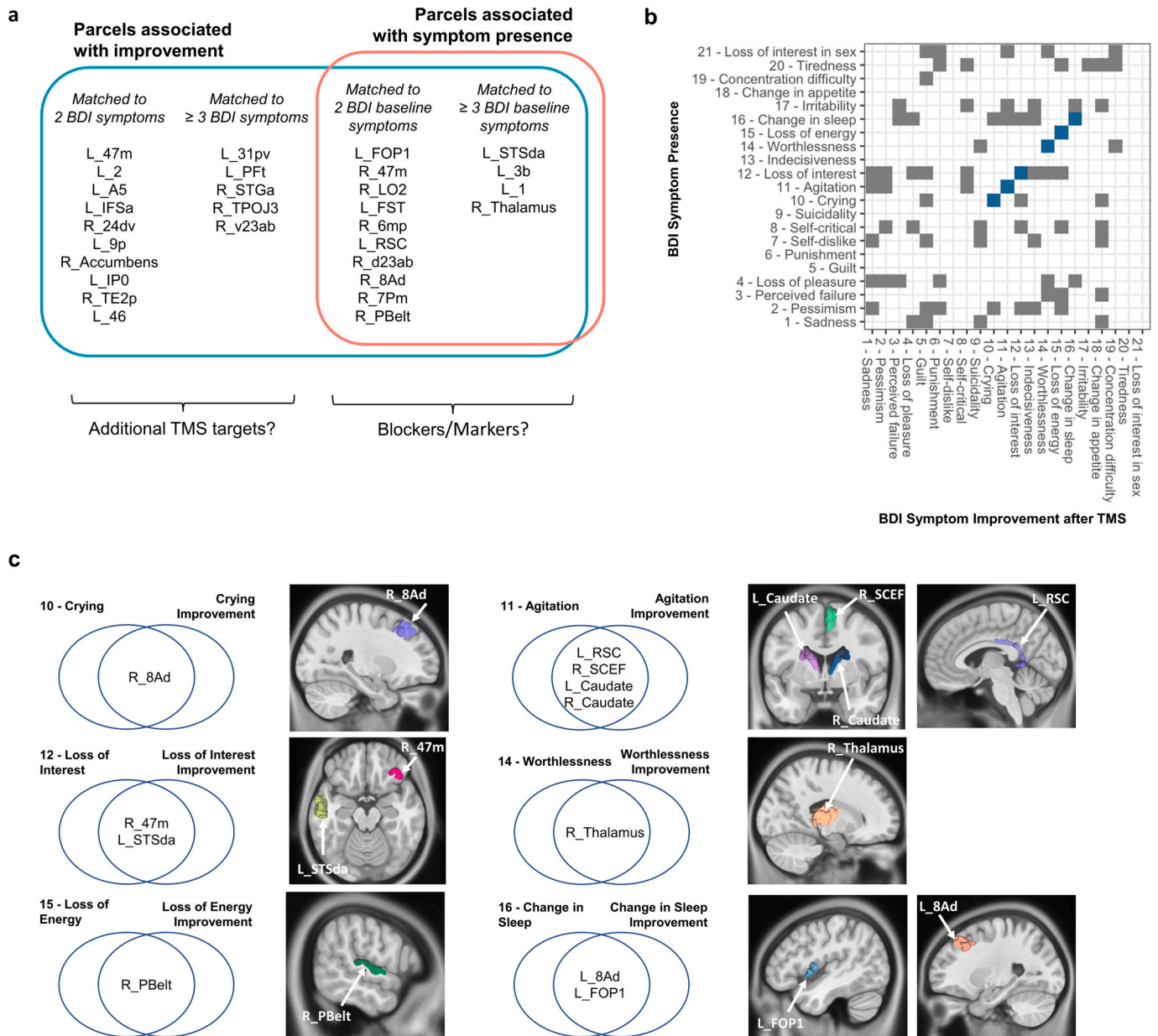


**Fig. 4.** The crossover of predictors of both symptom presence and response to treatment. The parcels that are associated with both may provide further targets for repetitive Transcranial Magnetic Stimulation. a) The parcels predicting resolution of at least two Beck's Depression Inventory items have been mapped in a Venn diagram. The parcels enclosed only by the blue box signify parcels which are only associated with symptom resolution, whereas parcels at the intersection of the blue and orange boxes are associated with at least two-fold symptom resolution but are also associated with presence of at least one symptom at baseline. b) The plot shows whether any parcels are associated with both presence and resolution of BDI-II items. The tiles in blue represent parcels which are associated with the presence and resolution of the same BDI-II item. c) The aforementioned blue tiles, parcels associated with the presence and resolution of the same BDI-II item have been mapped, showing their associated symptom, and anatomical location on T1-weighted magnetic resonance imaging. Six parcels are right sided, while four are left sided. (For interpretation of the references to colour in this figure legend, the reader is referred to the web version of this article.)

which may represent features of a distinct disease, not focused on the left BA46 or the salience network normally associated with depression, and which could be considered as additional or alternate targets in a non-traditional rTMS therapy. In our analysis, these potential additional/alternative targets may consist of the parcels which were only associated with symptom resolution. Alternatively, the machine learning models might be pointing out connectivity problems which might prevent the normalization of circuits with left DLPFC rTMS intervention – ‘blockers’ of treatment response to rTMS to area 46 which might need additional treatment or may make rTMS success unlikely. These parcels in our model may be those which were associated with both the presence and resolution of BDI-II items. These parcels may alternatively point to

features of the connectome which could predict treatment response to rTMS to left BA46, as well as physiological differences between TMS responders and non-responders. Given our relatively small sample size and examination of solely the baseline functional connectivity prior to treatment, a different interpretation of the role of these multiple symptom predictors is possible. Particularly, not knowing whether a region is overactive or underactive halts these hypotheses at a stage of speculation. While additional prospective data are necessary to confirm and substantiate the significance of our analysis, it seems likely that these kinds of questions are useful avenues for future inquiry.

The current study has inherent limitations. The small sample size limits the external validity of the findings and the confidence with which

the identified relationships can be applied clinically. Specifically, similar machine learning approaches typically require hundreds or thousands of data points to avoid over-fitting, however this is typically for models aimed at predicting beyond the limits of the data it is analyzing. It is important to note that the present study used machine learning to explore a novel relationship, which it is hoped will encourage future large-scale studies to consider utilizing similar approaches. Furthermore, we applied methods to protect against false conclusions from results produced by over-fitting our models within a small sample. This included the use of 5-fold cross validation, which controls for over-fitting within the model through the training of multiple models on different subsets of the data, then validating the performance of those trained models on several subsets of the already available data, and assessing the classification accuracy across the held-out data. Subsequently, because the classifiers across the 5-fold cross validations were still accurate, this lessens the likelihood that over-fitting of the model led to erroneous conclusions and predictions.

Additionally, the 3-week duration of rTMS treatment may also have been insufficient for all participants to show improvement, especially considering our approach which binarized the definition of symptom improvement as complete resolution to attain balanced class sizes given our small sample size. Some participants who were defined as non-responders may therefore not have been non-responders if longer treatment length had been applied, and the model instead may have identified features of the connectome associated with patients who are early responders to rTMS. These patients may however still be those who benefit the most from rTMS (37). The variation in rTMS protocol for patients (10 Hz on left DLPFC, 1 Hz on right DLPFC, or bilateral sequential) is a limitation, as a lack of stimulation to the same brain region for all participants for the whole treatment course reduces experimental consistency. Finally, the reproducibility and clinical utility of our machine learning model has not yet been evaluated. Our analysis also did not consider other possible confounds, including the role of pharmacotherapy. Prospective studies should examine these patterns with other depression inventories in larger samples and consider sham treatment and randomized designs. Nonetheless, machine learning tools such as ours have the potential to revolutionize precision medicine.

#### Role of the funding source

No funding was received to undergo this study.

#### CRediT authorship contribution statement

**Hugh Taylor:** Formal analysis, Investigation, Software. **Peter Nicholas:** Formal analysis, Validation, Software. **Kate Hoy:** Writing – review & editing, Data curation. **Neil Bailey:** Writing – review & editing, Data curation. **Onur Tanglay:** Writing – original draft. **Isabella M. Young:** Project administration, Writing – review & editing. **Lewis Dobbin:** Data curation, Formal analysis. **Stephane Doyen:** Conceptualization, Methodology. **Michael E. Sughrue:** Conceptualization. **Paul B. Fitzgerald:** Methodology, Supervision.

#### Conflict of interest

Seven authors (HT, PN, OT, IY, LD, SD and MS) are employees of Omniscient Neurotechnology. SD and MS are also stakeholders of Omniscient Neurotechnology.

#### Acknowledgements

We have no acknowledgements to declare.

#### Appendix A. Supplementary data

Supplementary data to this article can be found online at <https://doi.org/10.1016/j.jad.2023.02.082>.

[org/10.1016/j.jad.2023.02.082](https://doi.org/10.1016/j.jad.2023.02.082).

#### References

- Akiki, T.J., Abdallah, C.G., 2019. Determining the hierarchical architecture of the human brain using subject-level clustering of functional networks. *Biorxiv* 350462. <https://doi.org/10.1101/350462>.
- Amad, A., Fovet, T., 2022. rTMS for depression: the difficult transition from research to clinical practice. *Austral. N. Z. J. Psychiatry* 56, 14–15. <https://doi.org/10.1177/00048674211011242>.
- Bailey, N.W., Hoy, K.E., Rogasch, N.C., Thomson, R.H., McQueen, S., Elliot, D., Sullivan, C.M., Fulcher, B.D., Daskalakis, Z.J., Fitzgerald, P.B., 2018. Responders to rTMS for depression show increased fronto-midline theta and theta connectivity compared to non-responders. *Brain Stimul.* 11, 190–203. <https://doi.org/10.1016/j.brs.2017.10.015>.
- Beam, W., Borckardt, J.J., Reeves, S.T., George, M.S., 2009. An efficient and accurate new method for locating the F3 position for prefrontal TMS applications. *Brain Stimul.* 2, 50–54. <https://doi.org/10.1016/j.brs.2008.09.006>.
- Behzadi, Y., Restom, K., Liu, J., Liu, T.T., 2007. A component based noise correction method (CompCor) for BOLD and perfusion based fMRI. *Neuroimage* 37, 90–101. <https://doi.org/10.1016/j.neuroimage.2007.04.042>.
- Beuzon, G., Timour, Q., Saoud, M., 2017. Predictors of response to repetitive transcranial magnetic stimulation (rTMS) in the treatment of major depressive disorder. *L'Encéphale* 43, 3–9. <https://doi.org/10.1016/j.encep.2016.11.002>.
- Blom, E.H., Duncan, L.G., Ho, T.C., Connolly, C.G., LeWinn, K.Z., Chesney, M., Hecht, F.M., Yang, T.T., 2014. The development of an RDoC-based treatment program for adolescent depression: “Training for awareness, resilience, and action” (TARA). *Front. Hum. Neurosci.* 8, 630. <https://doi.org/10.3389/fnhum.2014.00630>.
- Cao, X., Deng, C., Su, X., Guo, Y., 2018. Response and remission rates following high-frequency vs. Low-frequency repetitive transcranial magnetic stimulation (rTMS) over right DLPFC for treating major depressive disorder (MDD): a meta-analysis of randomized, double-blind trials. *Frontiers. Psychiatry* 9, 413. <https://doi.org/10.3389/fpsy.2018.00413>.
- Cash, R.F.H., Zalesky, A., Thomson, R.H., Tian, Y., Cocchi, L., Fitzgerald, P.B., 2019. Subgenual functional connectivity predicts antidepressant treatment response to transcranial magnetic stimulation: independent validation and evaluation of personalization. *Biol. Psychiatry* 86, e5–e7. <https://doi.org/10.1016/j.biopsych.2018.12.002>.
- Cash, R.F.H., Weigand, A., Zalesky, A., Siddiqi, S.H., Downar, J., Fitzgerald, P.B., Fox, M.D., 2021. Using brain imaging to improve spatial targeting of transcranial magnetic stimulation for depression. *Biol. Psychiatry* 90, 689–700. <https://doi.org/10.1016/j.biopsych.2020.05.033>.
- Cieslik, E.C., Zilles, K., Caspers, S., Roski, C., Kellermann, T.S., Jakobs, O., Langner, R., Laird, A.R., Fox, P.T., Eickhoff, S.B., 2013. Is there “One” DLPFC in cognitive action Control? Evidence for heterogeneity from co-activation-based parcellation. *Cereb. Cortex* 23, 2677–2689. <https://doi.org/10.1093/cercor/bhs256>.
- Corlier, J., Wilson, A., Hunter, A., Vince-Cruz, N., Krantz, D., Levitt, J., Minzenberg, M., Ginder, N., Cook, I., Leuchter, A., 2019. Changes in functional connectivity predict outcome of repetitive transcranial magnetic stimulation treatment of major depressive disorder. *Brain Stimul.* 12, 548–549. <https://doi.org/10.1016/j.brs.2018.12.812>.
- Dalgleish, T., Black, M., Johnston, D., Bevan, A., 2020. Transdiagnostic approaches to mental health problems: current status and future directions. *J Consult Clin Psych* 88, 179–195. <https://doi.org/10.1037/ccp0000482>.
- Dinga, R., Schmaal, L., Penninx, B.W.J.H., Tol, M.J., van Veltman, D.J., Velzen, L., van Mennes, M., Wee, N.J.A. van der, Marquand, A.F., 2019. Evaluating the evidence for biotypes of depression: Methodological replication and extension of Drysdale et al. (2017). *Neuroimage Clin* 22, 101796. <https://doi.org/10.1016/j.nicl.2019.101796>.
- Doyen, S., Taylor, H., Nicholas, P., Crawford, L., Young, I., Sughrue, M.E., 2021. Hollow-tree super: a directional and scalable approach for feature importance in boosted tree models. *PLoS One* 16, e0258658. <https://doi.org/10.1371/journal.pone.0258658>.
- Doyen, S., Nicholas, P., Poologaindran, A., Crawford, L., Young, I.M., Romero-Garcia, R., Sughrue, M.E., 2022. Connectivity-based parcellation of normal and anatomically distorted human cerebral cortex. *Hum. Brain Mapp.* 43, 1358–1369. <https://doi.org/10.1002/hbm.25728>.
- Drysdale, A.T., Grosenick, L., Downar, J., Dunlop, K., Mansouri, F., Meng, Y., Fetcho, R.N., Zebley, B., Oathes, D.J., Etkin, A., Schatzberg, A.F., Sudheimer, K., Keller, J., Mayberg, H.S., Gunning, F.M., Alexopoulos, G.S., Fox, M.D., Pascual-Leone, A., Voss, H.U., Casey, B., Dubin, M.J., Liston, C., 2017. Resting-state connectivity biomarkers define neurophysiological subtypes of depression. *Nat. Med.* 23, 28–38. <https://doi.org/10.1038/nm.4246>.
- Eshel, N., Keller, C.J., Wu, W., Jiang, J., Mills-Finnerty, C., Huemer, J., Wright, R., Fonzo, G.A., Ichikawa, N., Carreon, D., Wong, M., Yee, A., Shpigel, E., Guo, Y., McTeague, L., Maron-Katz, A., Etkin, A., 2020. Global connectivity and local excitability changes underlie antidepressant effects of repetitive transcranial magnetic stimulation. *Neuropsychopharmacol.* 45, 1018–1025. <https://doi.org/10.1038/s41386-020-0633-z>.
- Fitzgerald, P.B., 2021. Targeting repetitive transcranial magnetic stimulation in depression: do we really know what we are stimulating and how best to do it? *Brain Stimul.* 14, 730–736. <https://doi.org/10.1016/j.brs.2021.04.018>.
- Fitzgerald, P.B., Benitez, J., de Castella, A., Daskalakis, Z.J., Brown, T.L., Kulkarni, J., 2006. A randomized, controlled trial of sequential bilateral repetitive transcranial magnetic stimulation for treatment-resistant depression. *Am. J. Psychiatry* 163, 88–94. <https://doi.org/10.1176/appi.ajp.163.1.88>.

- Fitzgerald, P.B., Hoy, K., McQueen, S., Maller, J.J., Herring, S., Segrave, R., Bailey, M., Been, G., Kulkarni, J., Daskalakis, Z.J., 2009. A randomized trial of rTMS targeted with MRI based neuro-navigation in treatment-resistant depression. *Neuropsychopharmacol* 34, 1255–1262. <https://doi.org/10.1038/npp.2008.233>.
- Fox, M.D., Buckner, R.L., White, M.P., Greicius, M.D., Pascual-Leone, A., 2012. Efficacy of transcranial magnetic stimulation targets for depression is related to intrinsic functional connectivity with the subgenual cingulate. *Biol Psychiat* 72, 595–603. <https://doi.org/10.1016/j.biopsych.2012.04.028>.
- Gellersen, H.M., Kedzior, K.K., 2019. Antidepressant outcomes of high-frequency repetitive transcranial magnetic stimulation (rTMS) with F8-coil and deep transcranial magnetic stimulation (DTMS) with H1-coil in major depression: a systematic review and meta-analysis. *BMC Psychiatry* 19, 139. <https://doi.org/10.1186/s12888-019-2106-7>.
- Glasser, M.F., Coalson, T.S., Robinson, E.C., Hacker, C.D., Harwell, J., Yacoub, E., Ugurbil, K., Andersson, J., Beckmann, C.F., Jenkinson, M., Smith, S.M., Essen, D.C.V., 2016. A multi-modal parcellation of human cerebral cortex. *Nature* 536, 171–178. <https://doi.org/10.1038/nature18933>.
- Hasanzadeh, F., Mohebbi, M., Rostami, R., 2019. Prediction of rTMS treatment response in major depressive disorder using machine learning techniques and nonlinear features of EEG signal. *J. Affect. Disord.* 256, 132–142. <https://doi.org/10.1016/j.jad.2019.05.070>.
- Jenkinson, M., Beckmann, C.F., Behrens, T.E.J., Woolrich, M.W., Smith, S.M., 2012. FSL. *Neuroimage* 62, 782–790. <https://doi.org/10.1016/j.neuroimage.2011.09.015>.
- Kaster, T.S., Downar, J., Vila-Rodriguez, F., Thorpe, K.E., Feffer, K., Noda, Y., Giacobbe, P., Knyahnytska, Y., Kennedy, S.H., Lam, R.W., Daskalakis, Z.J., Blumberger, D.M., 2019. Trajectories of response to dorsolateral prefrontal rTMS in major depression: a THREE-D study. *Am J Psychiat* 176, 367–375. <https://doi.org/10.1176/appi.ajp.2018.18091096>.
- Li, Y., Wang, L., Jia, M., Guo, J., Wang, H., Wang, M., 2017. The effects of high-frequency rTMS over the left DLPFC on cognitive control in young healthy participants. *PLoS One* 12, e0179430. <https://doi.org/10.1371/journal.pone.0179430>.
- Ma, N., Liu, Y., Li, N., Wang, C.-X., Zhang, H., Jiang, X.-F., Xu, H.-S., Fu, X.-M., Hu, X., Zhang, D.-R., 2010. Addiction related alteration in resting-state brain connectivity. *NeuroImage* 49, 738–744. <https://doi.org/10.1016/j.neuroimage.2009.08.037>.
- Muhle-Karbe, P.S., Derrfuss, J., Lynn, M.T., Neubert, F.X., Fox, P.T., Brass, M., Eickhoff, S.B., 2016. Co-activation-based parcellation of the lateral prefrontal cortex delineates the inferior frontal junction area. *Cereb. Cortex* 26, 2225–2241. <https://doi.org/10.1093/cercor/bhv073>.
- Risio, L.D., Borgi, M., Pettoruso, M., Miuli, A., Ottomana, A.M., Sociali, A., Martinotti, G., Nicolò, G., Macrì, S., di Giannantonio, M., Zoratto, F., 2020. Recovering from depression with repetitive transcranial magnetic stimulation (rTMS): a systematic review and meta-analysis of preclinical studies. *Transl Psychiat* 10, 393. <https://doi.org/10.1038/s41398-020-01055-2>.
- Rosen, A.C., Bhat, J.V., Cardenas, V.A., Ehrlich, T.J., Horwege, A.M., Mathalon, D.H., Roach, B.J., Glover, G.H., Badran, B.W., Forman, S.D., George, M.S., Thase, M.E., Yurgelun-Todd, D., Sughrue, M.E., Doyen, S.P., Nicholas, P.J., Scott, J.C., Tian, L., Yesavage, J.A., 2021. Targeting location relates to treatment response in active but not sham rTMS stimulation. *Brain Stimul.* 14, 703–709. <https://doi.org/10.1016/j.brs.2021.04.010>.
- Siddiqi, S.H., Trapp, N.T., Shahim, P., Hacker, C.D., Laumann, T.O., Kandala, S., Carter, A.R., Brody, D.L., 2019. Individualized connectome-targeted transcranial magnetic stimulation for neuropsychiatric sequelae of repetitive traumatic brain injury in a retired NFL player. *J. Neuropsychiatry Clin. Neurosci.* 31, 254–263. <https://doi.org/10.1176/appi.neuropsych.18100230>.
- Taylor, S.F., Ho, S.S., Abagis, T., Angstadt, M., Maixner, D.F., Welsh, R.C., Hernandez-Garcia, L., 2018. Changes in brain connectivity during a sham-controlled, transcranial magnetic stimulation trial for depression. *J. Affect Disord.* 232, 143–151. <https://doi.org/10.1016/j.jad.2018.02.019>.
- Weigand, A., Horn, A., Caballero, R., Cooke, D., Stern, A.P., Taylor, S.F., Press, D., Pascual-Leone, A., Fox, M.D., 2018. Prospective validation that subgenual connectivity predicts antidepressant efficacy of transcranial magnetic stimulation sites. *Biol. Psychiatry* 84, 28–37. <https://doi.org/10.1016/j.biopsych.2017.10.028>.
- Yeo, B.T.T., Krienen, F.M., Sepulcre, J., Sabuncu, M.R., Lashkari, D., Hollinshead, M., Roffman, J.L., Smoller, J.W., Zöllei, L., Polimeni, J.R., Fischl, B., Liu, H., Buckner, R.L., 2011. The organization of the human cerebral cortex estimated by intrinsic functional connectivity. *J. Neurophysiol.* 106, 1125–1165. <https://doi.org/10.1152/jn.00338.2011>.